arXiv:2110.07258v2 [gr-qc] 28 Jan 2022

Constraints on Barrow entropy from M87* and S2 star observations

Kimet Jusufi,[1,*] Mustapha Azreg-Aïnou,[2,†] Mubasher Jamil,[3,4,‡] and Emmanuel N. Saridakis[5,6,§]

[1] *Physics Department, State University of Tetovo, Ilinden Street nn, 1200, Tetovo, North Macedonia*
[2] *Engineering Faculty, Başkent University, Bağlıca Campus, 06790-Ankara, Turkey*
[3] *Institute for Theoretical Physics and Cosmology, Zhejiang University of Technology, Hangzhou 310023 China*
[4] *School of Natural Sciences, National University of Sciences and Technology, Islamabad, 44000, Pakistan*
[5] *National Observatory of Athens, Lofos Nymfon, 11852 Athens, Greece*
[6] *CAS Key Laboratory for Researches in Galaxies and Cosmology, Department of Astronomy, University of Science and Technology of China, Hefei, Anhui 230026, P.R. China*

We use data from M87* central black hole shadow, as well as from the S2 star observations, in order to extract constraints on Barrow entropy. The latter is a modified entropy arising from quantum-gravitational effects on the black hole horizon, quantified by the new parameter Δ. Such a change in entropy leads to a change in temperature, as well as to the properties of the black hole and its shadow. We investigate the photon sphere and the shadow of a black hole with Barrow entropy, and assuming a simple model for infalling and radiating gas we estimate the corresponding intensity. Furthermore, we use the radius in order to extract the real part of the quasinormal modes, and for completeness we investigate the spherical accretion of matter onto the black hole, focusing on isothermal and polytropic test fluids. We extract the allowed parameter region, and by applying a Monte-Carlo-Markov Chains analysis we find that $\Delta \simeq 0.0036^{+0.0792}_{-0.0145}$. Hence, our results place the upper bound $\Delta \lesssim 0.0828$ at 1σ, a constraint that is less strong than the Big Bang Nucleosynthesis one, but significantly stronger than the late-time cosmological constraints.

I. INTRODUCTION

Black holes are currently the leading astrophysical laboratories for testing general relativity as well as theories of modified and quantum gravity. In particular, recent advances in optical, radio, X-ray and gravitational wave astronomy [1–3] have confirmed the presence of supermassive black holes in the galactic centers of giant elliptical and spiral galaxies, as well as small astrophysical black holes. Due to the observation of the first radio images of the supermassive black hole that exists at the center of the M87* galaxy, by Event Horizon Telescope (EHT), black-hole shadows have become a very useful tool to test general relativity and examine whether possible deviations due to gravitational modifications [4, 5] could indeed be the case. In such researches, one first calculates the shadows of various black hole solutions [6–37] and then confronts them with the M87* data [38–65].

On the other hand, one of the most intriguing discoveries is the theoretical connection between thermodynamics and gravity, which may play a significant role to understand more deeply the nature of black holes. In the classical relativistic picture, black holes can decrease the entropy of the universe by swallowing objects and therefore violating the second law of thermodynamics. To resolve this problem, Bekenstein [66] conjectured that black holes should have entropy. This idea was shown by Hawking using the semi-classical approach to be correct, and it was found that black holes radiate away energy and consequently the external observer would associate a temperature to the black hole horizon [67]. The laws of black hole thermodynamics relate the horizon temperature with the surface gravity. Hence, the black hole entropy, namely the Bekenstein-Hawking entropy, is given by $S_B = A/4$, where S_B is the entropy and A the surface area of the black hole (in units where $\hbar = G = c = 1$).

Recently, Barrow argued that quantum-gravitational effects induce a fractal structure on the black hole horizon, which then acquires spatial dimension more than two but less than three, quantified by the parameter Δ [68]. Hence, such a complex structure leads to a modification of the black hole entropy. This idea may have interesting consequences in cosmological and holographic applications [69–80]. Nevertheless, it also has interesting implications on the black hole properties itself, since it changes the black hole temperature too [81–83].

In this work we are interested in extracting constraints on the Barrow exponent Δ, using data form the M87* central black hole shadow, as well as from the S2 star observations. The manuscript is organized as follows. In Sec. II, we review Barrow entropy. In Sec. III we apply the involved expressions in order to find the black hole properties and the shadow images. Moreover, in Sec. IV we use the M87* observations and we analyze the motion of the S2 star orbit to fit the data and improve the constraints on the Barrow parameter. Finally, in Sec. V we conclude. For completeness, in the Appendix we consider the spherical accretion of isothermal and polytropic fluids onto black holes with Barrow entropy.

* kimet.jusufi@unite.edu.mk
† azreg@baskent.edu.tr
‡ mjamil@zjut.edu.cn
§ msaridak@phys.uoa.gr

II. BLACK HOLES WITH BARROW ENTROPY

Barrow proposed a modification of Bekenstein-Hawking black hole entropy induced by quantum gravity effects on its horizon [68]. The corresponding corrections change the exponent of the entropy-area law, leading to

$$S_B = \left(\frac{A}{4}\right)^{1+\frac{\Delta}{2}}, \tag{1}$$

where Δ is the new parameter, and with A the usual area of the black hole's event horizon. Δ is restricted to the interval $0 \leq \Delta \leq 1$, with $\Delta = 0$ giving the standard Bekenstein–Hawking entropy, while $\Delta = 1$ corresponding to the maximal deformation of the horizon structure.

In this work we will focus on Schwarzschild black hole solutions, with metric

$$ds^2 = -f(r)dt^2 + \frac{dr^2}{f(r)} + r^2\left(d\theta^2 + \sin^2\theta d\phi^2\right). \tag{2}$$

If the mass parameter is M, the corresponding horizon is $r_H = 2M$, and as usual we can express its area as $A = 4\pi r_H^2 = 16\pi M^2$. In this case (1) can be re-written as $S_B(M) = \left(4\pi M^2\right)^{1+\frac{\Delta}{2}}$. Hence, using that $\frac{1}{T} = \frac{\partial S_B}{\partial M}$, one can find the modified black hole temperature [84] arising from the modified Barrow entropy as [81]

$$T_B = \frac{1}{(\Delta+2)(4\pi)^{1+\frac{\Delta}{2}} M^{1+\Delta}}. \tag{3}$$

In summary, the effect of Barrow entropy is to change the black hole temperature too, while in the case $\Delta = 0$ we re-obtain the standard Hawking temperature $T = 1/(8\pi M)$.

Let us proceed by considering a standard Schwarzschild black hole solution that would have the same temperature with the above Barrow temperature. Using the well-known expression for the black hole temperature $T = \frac{f'(r)}{4\pi}|_{r=\tilde{r}_H}$, with $\tilde{r}_H$ the horizon, we can easily see that in this case the corresponding metric function should be

$$f(r) = 1 - \frac{(\Delta+2)M^{\Delta+1}(4\pi)^{\frac{\Delta}{2}}}{r}, \tag{4}$$

and thus the horizon should be

$$\tilde{r}_H = (4\pi)^{\frac{\Delta}{2}}(\Delta+2)M^{\Delta+1}, \tag{5}$$

and the mass

$$\tilde{M} = (4\pi)^{\frac{\Delta}{2}}\left(\frac{\Delta}{2}+1\right)M^{\Delta+1}. \tag{6}$$

In the limiting case where Barrow entropy becomes standard Bekenstein-Hawking entropy, i.e for $\Delta = 0$, the above solution becomes the standard one.

Now, it is well known that the Hawking temperature can be also understood geometrically by Wick-rotating the time coordinate $t \to i\tau$ and $r \to \tilde{r}_H + \delta r$. Thus,

$$f(r) = \frac{r - \tilde{r}_H}{r}, \tag{7}$$

and then near the horizon we have $f(r) \simeq f'(r)|_{\tilde{r}_H}(r - \tilde{r}_H)$, and the metric (2) reads [84]

$$ds^2 = \frac{\delta r^2}{\tilde{r}_H}d\tau^2 + \frac{\tilde{r}_H}{\delta r}d(\delta r)^2 + \tilde{r}_H^2\left(d\theta^2 + \sin^2\theta d\phi^2\right). \tag{8}$$

Defining a new radial coordinate ρ as $\rho = 2\sqrt{\tilde{r}_H \delta r}$, the line element acquires the form

$$ds^2 \simeq \frac{\rho^2}{4\tilde{r}_H^2}d\tau^2 + d\rho^2 + \tilde{r}_H^2\left(d\theta^2 + \sin^2\theta d\phi^2\right). \tag{9}$$

In order to avoid the conical singularity we can impose the periodicity of the Euclidean time coordinate τ as

$$\frac{\tau}{2\tilde{r}_H} \sim \frac{\tau}{2\tilde{r}_H} + 2\pi, \tag{10}$$

and then we can identify the inverse of the period of the Euclidean time coordinate to correspond to the temperature [84]. In particular, in the Euclidean path integral formulation we can make the identification for the finite temperature field theory using the relation

$$\int [D\phi]\, \mathrm{e}^{\int_0^{t_0} dt\, L(\phi)} = \mathrm{Tr}\left(\mathrm{e}^{-t_0 H}\right) = \mathrm{Tr}\left(\mathrm{e}^{-\frac{H}{T}}\right), \tag{11}$$

which holds for any field ϕ, with which one finds that the Schwarzschild black hole (2) has temperature $T = 1/(4\pi\tilde{r}_H)$, which using (5) gives exactly a Hawking temperature that coincides with (3).

III. BARROW ENTROPY EFFECT ON BLACK HOLE SHADOWS

In this section we use the Schwarzschild-like metric which we found by using the Barrow corrected black hole temperature in order to study the shadow of a black hole possessing Barrow entropy. As it is known, there are two constants of motion for particle motion in spherically symmetric geometry, due to the existence of the timelike and spacelike Killing vectors, namely the energy E and the angular momentum L of the particle, in our case photon, respectively. Following the standard procedure it is straightforward to obtain the equations of motion for the photon [12]

$$\frac{dt}{d\lambda} = \frac{E}{f(r)}, \tag{12}$$

$$\frac{dr}{d\lambda} = \frac{\sqrt{R(r)}}{r^2}, \tag{13}$$

$$\frac{d\theta}{d\lambda} = \frac{\sqrt{\Theta(\theta)}}{r^2}, \tag{14}$$

$$\frac{d\phi}{d\lambda} = \frac{L\csc^2\theta}{r^2}, \tag{15}$$

where

$$R(r) \equiv E^2 r^4 - (\mathcal{K} + L^2) r^2 f(r), \tag{16}$$
$$\Theta(\theta) \equiv \mathcal{K} - L^2 \csc^2\theta \cos^2\theta, \tag{17}$$

where $\mathcal{K}$ is a constant of integration known as the Cartan constant. It simply follows from the separation of the Hamilton-Jacobi equations into a radial part and a polar part setting each part equal to $\mathcal{K}$ [85]. Using the above equations we can further study the radial geodesics by introducing the effective potential $V_{\rm eff}(r)$ as follows

$$\left(\frac{dr}{d\lambda}\right)^2 + V_{\rm eff}(r) = 0, \tag{18}$$

where

$$V_{\rm eff}(r) = -1 + \frac{f(r)}{r^2}(\xi^2 + \eta), \tag{19}$$

and

$$\xi = \frac{L}{E}, \quad \eta = \frac{\mathcal{K}}{E^2}. \tag{20}$$

We can use the two parameters ξ and η in order to analyze the motion of photons around the black hole. Since we are interested to explore the effect of the Barrow parameter on the shadow of the black hole, we need to use the conditions for unstable orbit. As we know, in the observer's sky, we can observe the black hole shadow due to the fact that some of the scattered photons escape from the black hole and some of the photons are captured by the black hole geometry. In other words, the black hole shadow is obtained as a union of the dark spots in the observer's sky. While it is straightforward to see that the critical orbits are characterized by certain critical values in terms of the impact parameters ξ and η. To determine the critical orbits or the unstable circular photon orbits, we simply need to study the effective potential, that is we need to find the maximum of the effective potential $V_{\rm eff}$ yielding the unstable orbits. Thees unstable circular photon orbits can be obtained by applying the following conditions:

$$V_{\rm eff} = 0, \quad V'_{\rm eff}(r) = 0, \quad V''_{\rm eff}(r) \leq 0.$$

Using Eqs. (13) and (18) it is easy to combine $V_{\rm eff}$ and $R(r)$. If we express the above conditions in terms of $R(r)$ we obtain:

$$R(r) = 0, \quad \frac{dR(r)}{dr} = 0, \quad \frac{d^2R(r)}{dr^2} > 0. \tag{21}$$

In terms of the above conditions one can easily show that the photon radius is determined by the following algebraic condition

$$2f(r) - rf'(r) = 0. \tag{22}$$

By solving (22) under (4), we obtain a simple relation for the radius of the photon sphere $r_{\rm ph}$ given by

$$r_{\rm ph} = \frac{3}{2}(2+\Delta) M^{\Delta+1} (4\pi)^{\frac{\Delta}{2}} = \frac{3}{2}\tilde{r}_H. \tag{23}$$

The radius of the photon sphere can be used to find the size of black hole shadow. In order to describe the shadow as seen by large distances, one introduces the two celestial coordinates X and Y [85], namely $X = \lim_{r_*\to\infty}\left(-r_*^2 \sin\theta_0 \frac{d\phi}{dr}\right)$ and $Y = \lim_{r_*\to\infty} r_*^2 \frac{d\theta}{dr}$, with r_* the distance between the black hole and the observer, and θ_0 the inclination angle between the observer's line of sight and the black hole rotational axis. Using the geodesics equations we finally obtain [86]

$$X = -\xi(r_{\rm ph}) \csc\theta_0 \ , \tag{24}$$
$$Y = \sqrt{\eta(r_{\rm ph}) - \xi^2(r_{\rm ph}) \cot^2\theta_0} \ , \tag{25}$$

and thus we have $X^2 + Y^2 = \xi^2(r_{\rm ph}) + \eta(r_{\rm ph})$. Hence, the event horizon (i.e. shadow) radius $R_{\rm sh}$ can finally be found as [12]

$$R_{\rm sh}(r_{\rm ph}) = \sqrt{\xi^2(r_{\rm ph}) + \eta(r_{\rm ph})} = \frac{r_{\rm ph}}{\sqrt{f(r_{\rm ph})}}, \tag{26}$$

which explicitly yields

$$R_{\rm sh} = 3\sqrt{3}\,(\Delta+2)\, 2^{\Delta-1} M^{\Delta+1} (4\pi)^{\frac{\Delta}{2}} \ . \tag{27}$$

We can see that the event horizon radius is expected to increase due to the effect of quantum gravity corrections, since $M > 0$ and $\Delta \geq 0$.

We continue by using the inverse relationship between $R_{\rm sh}$ and the real part of quasinormal modes given by [87, 88]

$$\omega_{\Re} = \lim_{l\gg 1} \frac{l+\frac{1}{2}}{R_{\rm sh}}, \tag{28}$$

with l the multipole numbers, which in our case gives

$$\omega_{\Re} = \lim_{l\gg 1} \frac{l+\frac{1}{2}}{3\sqrt{3}\,(\Delta+2)\, 2^{\Delta-1} M^{\Delta+1} (4\pi)^{\frac{\Delta}{2}}}. \tag{29}$$

In Table I we present the numerical values for the photon

Δ	$r_{\rm ph}$	$R_{\rm sh}$	$\omega_{\Re}$
0	3	5.196152424	0.5000000000
0.001	3.005300838	5.205333745	0.4991180853
0.005	3.026590476	5.242208479	0.4956071896
0.008	3.042648663	5.270022075	0.4929915236
0.010	3.053397641	5.288639851	0.4912560290
0.030	3.162827055	5.478177156	0.4742592542
0.050	3.275860255	5.673956398	0.4578949904
0.080	3.452414952	5.979758107	0.4344784798
0.100	3.574958849	6.192010363	0.4195852494
0.120	3.701516690	6.411214974	0.4052392912
0.150	3.899154632	6.753533931	0.3846987723
0.170	4.036303659	6.991083014	0.3716271436
0.200	4.250450140	7.361995599	0.3529037985

TABLE I. The photon sphere radius $r_{\rm ph}$, the event horizon radius $R_{\rm sh}$ and the real part of quasinormal modes $\omega_{\Re}$, for different values of Δ, with $M = 1$ and $l = 1$.

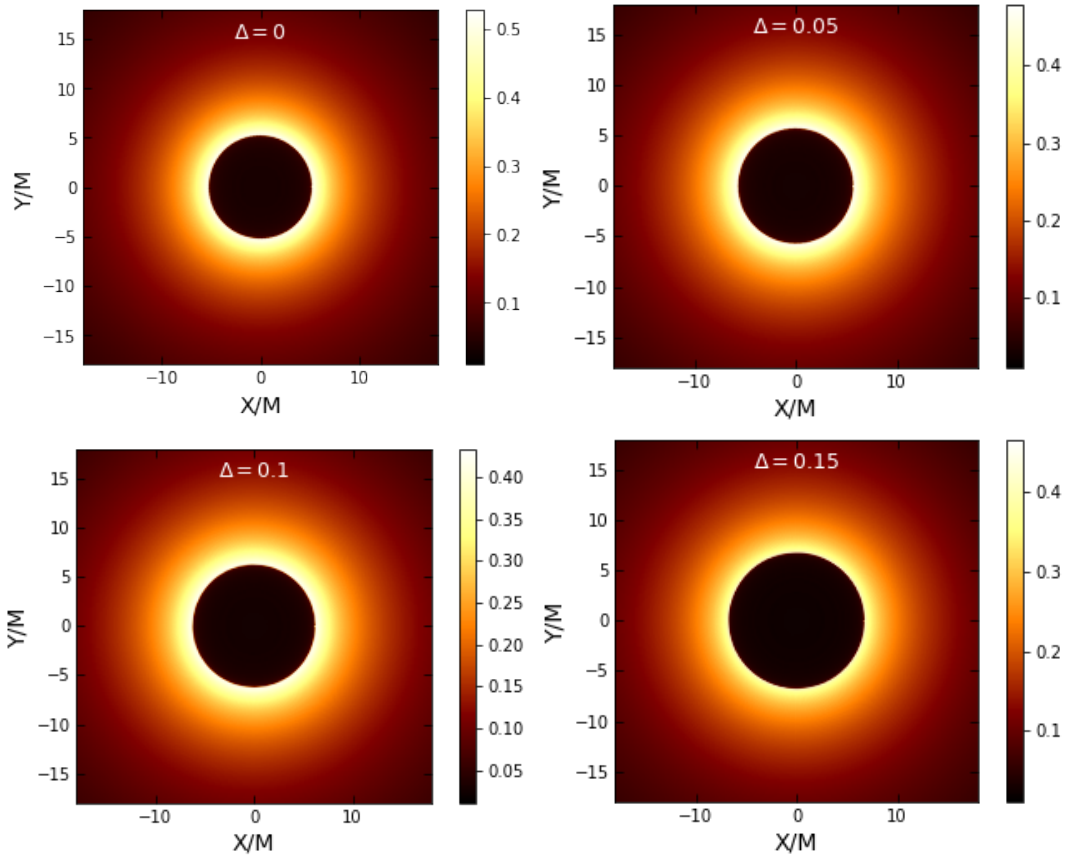


FIG. 1. *The shadow images and intensities for various values of Barrow exponent* Δ*, for fixed* $M = 1$.

radius, the values for the shadow radius, and the real part of quasinormal modes by varying the Barrow parameter. One can see that while the shadow radius increases by increasing Δ, the value of $\omega_{\Re}$ decreases. As we already mentioned, relation (29) is precise in the eikonal limit, namely $l \to \infty$, however it has been shown that in many cases it gives satisfactory results even for small l, which are most important for observations [87, 88]. Finally, the decrease in $\omega_{\Re}$ is therefore simply explained from the inverse relation between the real part of the quasinormal modes and the shadow radius, according to (28).

We close this section by considering the scenario where the black hole is surrounded by an infalling/radiating accretion flow. Via this simple model, we can extract valuable information about the intensity of the radiation which can be detected by a distant observer. In order to achieve this we need to estimate the specific intensity at the observed photon frequency $\nu_{\rm obs}$ at the point (X, Y) of the observer's image [37, 47, 89–92]

$$I_{obs}(\nu_{obs}, X, Y) = \int_{\gamma} \mathrm{g}^3 j(\nu_e) dl_{\rm prop}. \tag{30}$$

The freely falling gas has the four-velocity components written as

$$u_e^{\mu} = \left(\frac{1}{f(r)}, -\sqrt{1 - f(r)}, 0, 0\right), \tag{31}$$

with $f(r)$ given in (4). In addition we need to use the condition $p_\mu p^\mu = 0$, from which one can easily show that

$$\frac{p^r}{p^t} = \pm f(r)\sqrt{f(r)\left(\frac{1}{f(r)} - \frac{b^2}{r^2}\right)}, \tag{32}$$

with b the impact parameter. It is important to mention here that sign $+(-)$ describes the case when the photon approaches (or draws away) from the black hole. The redshift function g can be calculated using [37, 47, 89–92]

$$\mathrm{g} = \frac{p_\mu u^\mu_{obs}}{p_\nu u^\nu_e}, \tag{33}$$

with u^μ_{obs} the 4-velocity of the observer. For the specific emissivity we assume a simple model in which the emission is monochromatic, with emitter's-rest frame frequency $\nu_\star$, and the emission has a $1/r^2$ radial profile:

$$j(\nu_e) \propto \frac{\delta(\nu_e - \nu_\star)}{r^2}, \tag{34}$$

where δ denotes the Dirac delta function. Expressing the proper length in terms of radial coordinate for observed flux, we find

$$F_{obs}(X, Y) \propto -\int_{\gamma} \frac{\mathrm{g}^3 p_t}{r^2 p^r} dr. \tag{35}$$

In order to show all the above in a more transparent way, in Fig. 1 we present the black hole shadow for fixed M and various values of Barrow exponent Δ, according to (27). Additionally, we have numerically calculated and depicted the intensity from (35). As we observe, with increasing Barrow parameter the size of the shadow increases, while the intensity decreases.

Lastly, since we have extracted the black hole profile and properties we can straightforwardly investigate the accretion of matter onto it. For completeness, we provide this analysis in the Appendix.

IV. OBSERVATIONAL CONSTRAINTS ON THE BARROW PARAMETER

In this section we proceed to the use of the Event Horizon Telescope observations for the shadow of the M87* central black hole in order to impose constraints on the Barrow parameter Δ. As we will see, this will not be adequate and thus we need to incorporate additional data from the S2 star orbit observations [93, 94].

The M87* central black hole has angular diameter $\theta_{\rm sh} = (42 \pm 3)\mu as$, is at distance $D = 16.8$ Mpc, and its mass is $(6.5 \pm 0.9) \times 10^9 M_{\odot}$. We equate this to $\tilde{M}$ given in (6) in terms of the parameters Δ and M. Thus, we treat M as a parameter and not the true mass of the system. From a theoretical point of view this can be advantageous, since spherical solutions may be modeled differently, where each theoretical model introduces a set of parameters that have to be constrained to fit observational data. In this work we model M87* as a Barrow quantum-corrected two-parameter black hole, while one could model it using alternative theories of gravity too (see e.g. [95, 96]).

Combining the observational parameters allows us to introduce the single quantity d_{M87*}, which accounts for the size of the M87*'s shadow in unit mass, as [48]

$$d_{M87} = \frac{D\,\theta_{\rm sh}}{M_{87}} = 11.0 \pm 1.5. \tag{36}$$

In particular within 1σ confidence level one has the range $9.5 \leq d_{M87} \leq 12.5$.

Let us now use the theoretically predicted shadows of the previous section, in order to calculate the predicted diameter per unit mass $d_{\rm sh}$ for black holes with Barrow entropy. In Fig. 2 we depict $d_{\rm sh}$ as a function of Δ, for fixed $M = 1$, alongside the observational bounds according to (36). Nevertheless, as one can see, in general the results depend on both Δ and M. Indeed, in Fig. 3 we present the parameter region which is consistent with M87* data. Additionally, in Fig. 4 we present the predicted combined diameter $d_{\rm sh}$ as a function of M and Δ.

In order to break the degeneracy, and constrain Δ more efficiently, we have to use the S2 star orbit data [93, 94]. In particular, using solution (4), we can study the motion

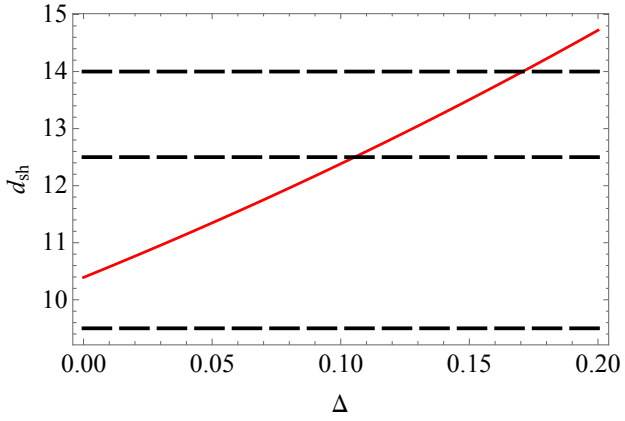


FIG. 2. *The theoretically predicted diameter per unit mass $d_{\rm sh}$, for black holes with Barrow entropy, as a function of Δ and for fixed $M = 1$. The horizontal dashed lines at 9.5 and 12.5 mark the 1σ bounds according to d_{M87*} observations, given in (36), while the horizontal dashed line at 14 marks the upper 2σ bound (the lower 2σ bound is not shown since it corresponds to the not physically interested region $\Delta < 0$).*

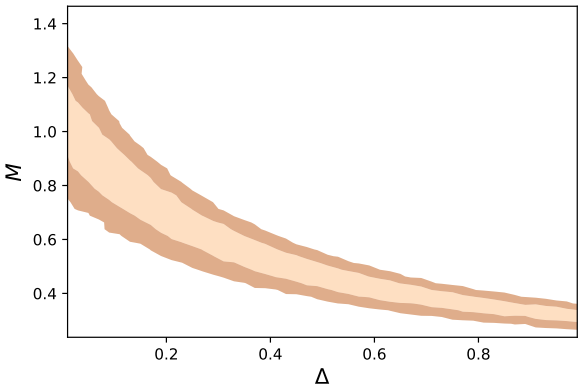


FIG. 3. *1σ and 2σ parameter region consistent with M87* shadow observations.*

of the S2 star restricted in the equatorial plane ($\theta = \pi/2,\ \dot{\theta} = 0$). From the Lagrangian it follows that

$$2\mathcal{L} = -f(r)\dot{t}^2 + \frac{\dot{r}^2}{f(r)} + r^2\dot{\phi}^2.$$

For the two constants of motion, namely total energy E and total angular momentum L of the star, we have $\frac{\partial \mathcal{L}}{\partial \dot{t}} = -E$ and $\frac{\partial \mathcal{L}}{\partial \dot{\phi}} = L$. Using the above we find that

$$\dot{t} = \frac{E}{1 - \frac{(\Delta+2)M^{\Delta+1}(4\pi)^{\frac{\Delta}{2}}}{r}}, \tag{37}$$

along with $\dot{\phi} = \frac{L}{r^2}$. Finally, we have the following equation of motion for a massive particle (S2 star in our case)

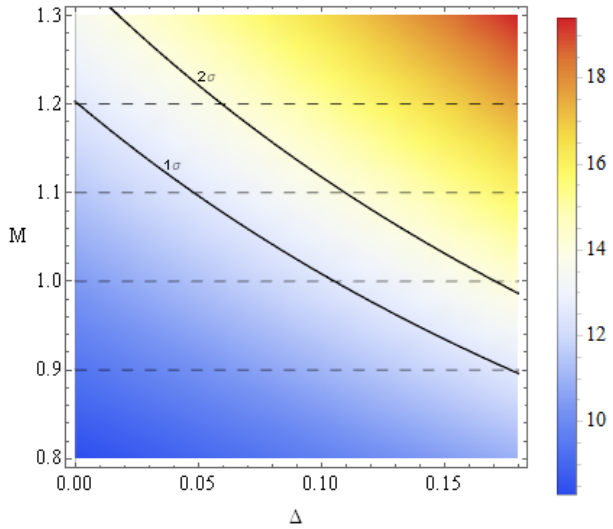


FIG. 4. *The predicted diameter per unit mass d, as a function of M and Δ. The black curves correspond to the observationally determined upper 1σ and 2σ bounds given in (36) (the lower ones are not shown since they correspond to the not physically interested region $\Delta < 0$).*

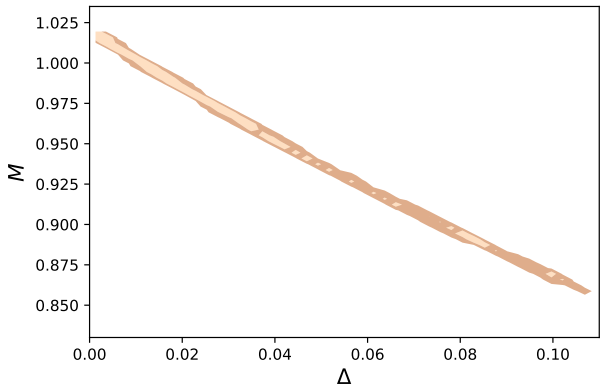


FIG. 5. *1σ and 2σ parameter region consistent with S2 star observations, after a Monte-Carlo-Markov Chains analysis.*

[97–99]

$$\ddot{r} = \frac{1}{2\, g_{11}(r)} \left[g_{00,r}(r)\, \dot{t}^2 + g_{11,r}(r)\, \dot{r}^2 + g_{33,r}(r)\dot{\phi}^2 \right]. \tag{38}$$

In general, one cannot find an analytical expression for $r(\phi)$ and, therefore, one must elaborate numerically the equations of motion. In the present work we apply the Bayesian theorem with the likelihood function as given in [99, 100], with the observational data for (X_{obs}, Y_{obs}) given in [94, 97], considering Δ and M as free parameters. In order to find the best-fit values we use the Monte-Carlo-Markov Chains analysis. For the central mass object we take $4.1 \times 10^6 M_\odot$ along with the uniform priors $0 < \Delta < 1$ and $0 < M < 2$. In Fig. 5 we present the region of the parameter space in agreement with S2 star data. Concerning Barrow parameter, in which we are interested in this manuscript, the best fit value and 1σ errors are

$$\Delta \simeq 0.0036^{+0.0792}_{-0.0145}, \tag{39}$$

which is the main result of the present work.

We can now combine the above result with the black hole shadow. In particular, applying the best-fit parameters we easily find the shadow radius $R_{\rm sh} = 5.3127$, measured in units of black hole mass. Hence, in Fig. 6 we depict the shadow image and intensity for a black hole with Barrow entropy, for the best-fit values of (39) and Fig. 5.

In summary, as we observe, although the standard value $\Delta = 0$, in which Barrow entropy becomes Bekenstein-Hawking entropy, lies inside the obtained 1σ region, the best-fit value is $\Delta = 0.0036$, while the 1σ upper bound is $\Delta \lesssim 0.0828$. Such constraint is stronger than the late-time cosmological ones from Supernovae (SNIa) Pantheon sample and cosmic chronometers (CC) datasets, namely $\Delta \lesssim 0.188$ [101, 102], but less strong than the Big Bang Nucleosynthesis (BBN) one, namely $\Delta \lesssim 1.4 \times 10^{-4}$ [103], since the latter is known to lead to very strong constraints. Hence, it reveals the capabilities of black hole shadow and S2 star observations, since they can lead to significantly improved constraints although the data points are for the currently relatively few.

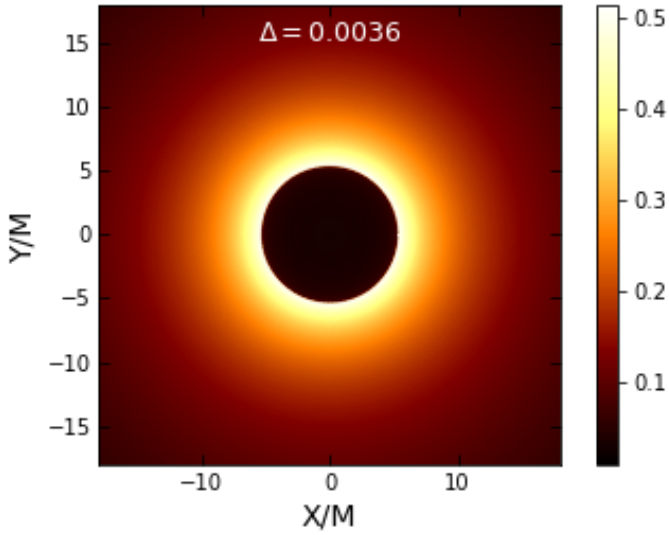


FIG. 6. *The shadow image and intensity for a black hole with Barrow entropy, for the best-fit values of (39) and Fig. 5 arising from S2 star data with Monte-Carlo-Markov Chains analysis.*

V. CONCLUSIONS

In this work we used data from M87* central black hole shadow, as well as from the S2 star observations, in order to extract constraints on Barrow entropy. The latter is a modified entropy relation arising from quantum-gravitational effects that induce a intricate, fractal structure on the black hole horizon, quantified by the new Barrow parameter Δ. Such a change in entropy leads to a change in temperature, as well as to the properties of the black hole and its shadow.

We investigated the photon sphere and the shadow of a black hole with Barrow entropy, and assuming a simple model for infalling and radiating gas we estimated the corresponding intensity. Furthermore, we used the radius in order to extract the real part of the quasinormal modes, and for completeness we investigated the spherical accretion of matter onto the black hole, focusing on isothermal and polytropic test fluids.

We used the EHT data from the M87* black hole extracting the allowed parameter region, and then we additionally incorporated data from the motion of S2 star around the Sgr A* black hole, through a Monte-Carlo-Markov Chains analysis, in order to break the degeneracies and extract the final constraints on the Barrow exponent. We found that $\Delta \simeq 0.0036^{+0.0792}_{-0.0145}$ at 1σ confidence level. Hence, our analysis places the upper bound $\Delta \lesssim 0.0828$, a constraint that is less strong than the Big Bang Nucleosynthesis (BBN) one, but significantly stronger than the late-time cosmological ones.

In summary, black-hole related data can serve as a new tool in order to test general relativity and examine if modifications of various kinds are allowed. Although the data points are currently few, they can be very efficient in constraining the theoretical parameters. The significant improvement of the datasets expected in the near future makes the corresponding analyses both interesting and necessary.

Although the M87* is shown and expected to rotate, the Sgr A* black hole might rotate very slowly compared to M87*. In most applications pertaining to Sgr A* rotation is dropped from consideration as in Refs. [98, 99, 113]. In that sense, the constraint we found for the S2 star is justified by assuming a nonrotating black hole in our galaxy. Rotation will be considered in a subsequent work.

Acknowledgements

ENS would like to acknowledge the contribution of the COST Action CA18108 "Quantum Gravity Phenomenology in the multi-messenger approach".

Appendix: Accretion of matter onto black holes with Barrow entropy

In this Appendix we investigate the accretion of matter onto black holes with Barrow entropy. We consider spherical accretion of a perfect fluid, whose stress-energy tensor is of the form $T^{\mu\nu} = (e+p)u^\mu u^\nu + pg^{\mu\nu}$, where e and p denotes the energy density and pressure, respectively. The black hole metric is assumed to be of the most general expression in spherical coordinates

$$ds^2 = -A(r)dt^2 + \frac{dr^2}{B(r)} + C(r)(d\theta^2 + \sin^2\theta d\phi^2). \quad \text{(A.1)}$$

The particle and energy conservation during the accretion procedure are $\nabla_\mu(nu^\mu) = 0$ and $\nabla_\mu T^{\mu\nu} = 0$ respectively, where $u^\mu = \frac{dx^\mu}{d\tau}$ is the four-velocity of the fluid particles (τ is the proper time) and n is the particle density. Introducing the three-velocity as [104] $v = \sqrt{\frac{1}{AB}}\frac{u^r}{u^t}$, and using the steps developed in [105–110], we obtain the location r_c of the critical point (CP) and the value of the corresponding three-velocity as

$$v_c^2 = a_c^2 \qquad \text{and} \qquad (1-a_c^2)\frac{A'}{A}\Big|_{r=r_c} = 2a_c^2\frac{C'}{C}\Big|_{r=r_c}, \quad \text{(A.2)}$$

where prime denotes derivative with respect to r, $v_c \equiv v|_{r=r_c}$, and with $a_c \equiv a|_{r=r_c}$ the three-dimensional speed of sound evaluated at the CP.

a. *Isothermal fluids*

The equation of state of an isothermal fluid is of the form $p = \omega e$ with $0 < \omega < 1$ a constant. Since the sound speed a is defined by $a^2 = dp/de$ we obtain $a^2 = \omega$, which depends of the particle's position within the fluid. Since a is constant, the second equation of (A.2) is easily solved knowing the metric (2),(4), namely with $A(r) = f(r)$ and $C(r) = r^2$, extracting the critical radius as

$$\tilde{r}_c = \left(3 + \frac{1}{a^2}\right)\frac{\tilde{r}_H}{4} = \left(3 + \frac{1}{a^2}\right)\frac{(4\pi)^{\frac{\Delta}{2}}(\Delta+2)M^{\Delta+1}}{4}. \quad \text{(A.3)}$$

Thus, for isothermal fluids a CP always exists since $\tilde{r}_c > \tilde{r}_H$ for $a^2 = \omega < 1$. Hence, the isothermal fluid reaches the sound speed before it is absorbed by the black hole horizon. When $\omega = 1/3 = a^2$, we have $\tilde{r}_c = 3\tilde{r}_H/2$ which is the location of the photon sphere. This correspondence is discussed later on.

b. *Polytropic fluids*

The polytropic equation of state is

$$p \propto n^\gamma, \qquad (\gamma > 1). \quad \text{(A.4)}$$

The corresponding sound speed takes the form [105, 106]

$$a^2 = \frac{(\gamma-1)\mathcal{X}}{m(\gamma-1)+\mathcal{X}}, \tag{A.5}$$

where $\mathcal{X} \propto n^{\gamma-1}$, and with m the baryonic mass. Due to the particle conservation the number density n is a function of $(r,\, v)$, and thus a^2 assumes the same dependence as n. This dependence was given in [105] leading to a complex relation between a^2 and $(r,\, v)$, namely

$$a^2 = \frac{\mathcal{Y}(\gamma-1)}{\left(\frac{1-v^2}{AC^2v^2}\right)^{\frac{1-\gamma}{2}} + \mathcal{Y}}, \tag{A.6}$$

where $\mathcal{Y} = \text{const.} > 0$ has dimensions of length to the power $2(\gamma-1)$, and depends on $(m,\, \gamma)$ and on the number density n_0 at some initial point (e.g. the spatial infinity or the CP [105]). In this case the solution of the second equation in (A.2) is still given by (A.3), but with a^2 replaced by a_c^2 since a^2 is no longer constant. Thus, reversing it we obtain

$$a_c^2 = \frac{\tilde{r}_H}{4\tilde{r}_c - 3\tilde{r}_H}. \tag{A.7}$$

It is usually admitted that $\gamma \leq 5/3$ and since (A.6) implies $a^2 < \gamma - 1 \leq 2/3$, we see from (A.3) that $\tilde{r}_c > \tilde{r}_H$ and thus a CP always exists provided the r.h.s. of (A.6) is positive and less than 1.

At the CP we have $v_c^2 = a_c^2$ given by the r.h.s. of (A.7). Substituting the above into (A.6) we obtain the following transcendental equation for $\tilde{r}_c$:

$$\frac{\tilde{r}_H}{4\tilde{r}_c - 3\tilde{r}_H} = \frac{\mathcal{Y}(\gamma-1)}{1+\mathcal{Y}\left(\frac{4}{\tilde{r}_H\tilde{r}_c^3}\right)^{(\gamma-1)/2}}\left(\frac{4}{\tilde{r}_H\tilde{r}_c^3}\right)^{(\gamma-1)/2}. \tag{A.8}$$

For the most used γ value in astrophysics, namely $\gamma = 5/3$, equation (A.8) can be solved explicitly as

$$\tilde{r}_c = \frac{9\times 2^{2/3}\mathcal{Y}}{2^{11/3}\mathcal{Y} - 3\tilde{r}_H^{4/3}}\,\tilde{r}_H. \tag{A.9}$$

To ensure that $\tilde{r}_c > \tilde{r}_H$ and $0 < a_c^2 < 1$ according to (A.7) we require $\mathcal{Y} > 3\tilde{r}_H^{4/3}/2^{11/3}$. This provides a constraint between the parameters on which $\mathcal{Y}$ depends and the parameters on which $\tilde{r}_H$ depends. The sound speed at the PC is obtained inserting (A.9) into (A.7), namely

$$a_c^2 = \frac{2^{11/3}\mathcal{Y} - 3\tilde{r}_H^{4/3}}{3\times 2^{8/3}\mathcal{Y} + 9\tilde{r}_H^{4/3}}, \tag{A.10}$$

with $\mathcal{Y} > 3\tilde{r}_H^{4/3}/2^{11/3}$. Since $\tilde{r}_H$ increases with Δ, from (A.9) we see that $\tilde{r}_c$ increases too (respectively a_c^2 decreases). Hence, as Δ increases the CP occurs at advanced positions where the fluid particles acquire a lower critical speed $v_c = a_c$.

c. Correspondence: The critical point versus the photon sphere

In order to determine the photon sphere for the general metric (A.1) we can repeat the steps of (12)-(22), finding that the radius of the photon sphere $r_{\rm ps}$ is determined by the equation [111, 112]

$$\frac{A'}{A}\Big|_{r=r_{\rm ps}} = \frac{C'}{C}\Big|_{r=r_{\rm ps}}, \tag{A.11}$$

which generalizes equation (22). Comparing (A.11) with the second equation in (A.2) we see that the location of the CP would correspond to the radius of the photon sphere if

$$1 - a_c^2 = 2a_c^2 \Rightarrow a_c^2 = \frac{1}{3}. \tag{A.12}$$

Since the sound speed $a^2 = dp/de$ is position-dependent, equation (A.12) would be satisfied only if at the CP the value of $a_c^2 = a^2|_{r=r_c}$ was just 1/3, which would mean that the CP occurs on the photon sphere.

There are special fluids where a^2 is constant and we may consider the value 1/3. This is indeed the case for the isothermal radiation fluid with an equation of state of the form $p = e/3$ resulting to $a^2 \equiv 1/3$. For such a fluid the CP always occurs on the photon sphere. However, for polytropic fluids, under specific conditions such a correspondence exists too. In particular, with $a_c^2 = 1/3$ from (A.7) we obtain $\tilde{r}_c = 3\tilde{r}_H/2$, and thus substituting into (A.8) we extract the condition on $\mathcal{Y}$ and $\tilde{r}_H$, namely

$$\tilde{r}_H^4 = \frac{32}{27}\left[(3\gamma-4)\mathcal{Y}\right]^{2/(\gamma-1)}, \tag{A.13}$$

alongside the previous condition (shown in (A.10) for the case $\gamma = 5/3$). Hence, for the case $\gamma = 5/3$ this reduces to

$$\tilde{r}_H^{4/3} = \frac{2^{5/3}}{3}\mathcal{Y} < \frac{2^{11/3}}{3}\mathcal{Y}, \tag{A.14}$$

which could be alternatively derived from (A.10) setting $a_c^2 = 1/3$. Equation (A.13) is a kind of fine-tuning condition between the parameters of the black hole, on the l.h.s., and the parameters of the polytropic fluid, on the r.h.s..

Hence, the sound speed at the critical point decreases with increasing Δ and thus the location of the critical point advances away from the black hole. For both fluids we can see that the critical point may occur on the photon sphere under specific conditions. For isothermal fluids only the sound speed is constrained, while for polytropic fluids both the black hole and the fluid parameters are constrained.

[1] B. P. Abbott *et al.* [LIGO Scientific and Virgo Collaborations], Phys. Rev. Lett. **116**, no. 6, 061102 (2016) [arXiv:1602.03837].

[2] K. Akiyama *et al.* [Event Horizon Telescope], Astrophys. J. Lett. **875**, L1 (2019) [arXiv:1906.11238].

[3] K. Akiyama *et al.* [Event Horizon Telescope], Astrophys. J. Lett. **875**, no.1, L2 (2019) [arXiv:1906.11239].

[4] E. N. Saridakis *et al.* [CANTATA], [arXiv:2105.12582].

[5] A. Addazi, J. Alvarez-Muniz, R. A. Batista, G. Amelino-Camelia, V. Antonelli, M. Arzano, M. Asorey, J. L. Atteia, S. Bahamonde and F. Bajardi, *et al.* [arXiv:2111.05659].

[6] R. Shaikh, Phys. Rev. D **100**, no. 2, 024028 (2019) [arXiv:1904.08322].

[7] S. W. Wei, Y. C. Zou, Y. X. Liu and R. B. Mann, JCAP **1908**, 030 (2019) [arXiv:1904.07710].

[8] J. W. Moffat and V. T. Toth, Phys. Rev. D **101**, no. 2, 024014 (2020) [arXiv:1904.04142].

[9] J. T. Firouzjaee and A. Allahyari, Eur. Phys. J. C **79**, no. 11, 930 (2019) [arXiv:1905.07378].

[10] I. Banerjee, B. Mandal and S. SenGupta, Phys. Rev. D **101**, no. 2, 024013 (2020) [arXiv:1905.12820].

[11] F. Long, J. Wang, S. Chen and J. Jing, JHEP **1910**, 269 (2019) [arXiv:1906.04456].

[12] T. Zhu, Q. Wu, M. Jamil and K. Jusufi, Phys. Rev. D **100**, no. 4, 044055 (2019) [arXiv:1906.05673].

[13] R. A. Konoplya and A. Zhidenko, Phys. Rev. D **100**, no. 4, 044015 (2019) [arXiv:1907.05551].

[14] E. Contreras, Á. Rincón, G. Panotopoulos, P. Bargueño and B. Koch, Phys. Rev. D **101**, no. 6, 064053 (2020) [arXiv:1906.06990].

[15] P. C. Li, M. Guo and B. Chen, Phys. Rev. D **101**, no. 8, 084041 (2020) [arXiv:2001.04231].

[16] R. Kumar, S. G. Ghosh and A. Wang, Phys. Rev. D **101**, no. 10, 104001 (2020) [arXiv:2001.00460].

[17] R. C. Pantig and E. T. Rodulfo, Chin. J. Phys. **68**, 236 (2020) [arXiv:2003.06829].

[18] S. V. M. C. B. Xavier, P. V. P. Cunha, L. C. B. Crispino and C. A. R. Herdeiro, Int. J. Mod. Phys. D **29**, no. 11, 2041005 (2020) [arXiv:2003.14349].

[19] M. Guo and P. C. Li, Eur. Phys. J. C **80**, no. 6, 588 (2020) [arXiv:2003.02523].

[20] R. Roy and S. Chakrabarti, Phys. Rev. D **102**, no. 2, 024059 (2020) [arXiv:2003.14107].

[21] X. H. Jin, Y. X. Gao and D. J. Liu, Int. J. Mod. Phys. D **29**, no. 09, 2050065 (2020) [arXiv:2004.02261].

[22] S. U. Islam, R. Kumar and S. G. Ghosh, JCAP **2009**, 030 (2020) [arXiv:2004.01038].

[23] C. Y. Chen, JCAP **05**, 040 (2020) [arXiv:2004.01440].

[24] R. A. Konoplya, J. Schee and D. Ovchinnikov, [arXiv:2008.04118].

[25] A. Belhaj, M. Benali, A. E. Balali, W. E. Hadri, H. El Moumni and E. Torrente-Lujan, [arXiv:2008.09908].

[26] F. Long, S. Chen, M. Wang and J. Jing, [arXiv:2009.07508].

[27] E. Contreras, Á. Rincón, G. Panotopoulos and P. Bargueño, [arXiv:2010.03734].

[28] W. H. Shao, C. Y. Chen and P. Chen, [arXiv:2011.07763].

[29] S. G. Ghosh, R. Kumar and S. U. Islam, [arXiv:2011.08023].

[30] K. Glampedakis and G. Pappas, [arXiv:2102.13573].

[31] R. A. Konoplya and A. Zhidenko, Phys. Rev. D **103**, no.10, 104033 (2021) [arXiv:2103.03855].

[32] H. M. Wang and S. W. Wei, [arXiv:2106.14602].

[33] M. Khodadi, G. Lambiase and D. F. Mota, JCAP **09**, 028 (2021) [arXiv:2107.00834].

[34] E. Frion, L. Giani and T. Miranda, [arXiv:2107.13536].

[35] Y. Zhu and T. Wang, [arXiv:2109.08463].

[36] M. Heydari-Fard, M. Heydari-Fard and H. R. Sepangi, Einstein-Maxwell-dilaton [arXiv:2110.02713].

[37] K. Jusufi and Saurabh, Mon. Not. Roy. Astron. Soc. **503**, 1310 (2021) [arXiv:2110.15870].

[38] H. Davoudiasl and P. B. Denton, Phys. Rev. Lett. **123**, no. 2, 021102 (2019) [arXiv:1904.09242].

[39] N. Bar, K. Blum, T. Lacroix and P. Panci, JCAP **1907**, 045 (2019) [arXiv:1905.11745].

[40] K. Jusufi, M. Jamil, P. Salucci, T. Zhu and S. Haroon, Phys. Rev. D **100**, no. 4, 044012 (2019) [arXiv:1905.11803].

[41] R. A. Konoplya, Phys. Lett. B **795**, 1 (2019) [arXiv:1905.00064].

[42] A. Narang, S. Mohanty and A. Kumar, [arXiv:2002.12786].

[43] S. Sau, I. Banerjee and S. SenGupta, Phys. Rev. D **102**, no. 6, 064027 (2020) [arXiv:2004.02840].

[44] A. Belhaj, M. Benali, A. El Balali, H. El Moumni and S. E. Ennadifi, Class. Quant. Grav. **37**, no. 21, 215004 (2020) [arXiv:2006.01078].

[45] R. Kumar, A. Kumar and S. G. Ghosh, Astrophys. J. **896**, no. 1, 89 (2020) [arXiv:2006.09869].

[46] X. X. Zeng and H. Q. Zhang, Eur. Phys. J. C **80**, no.11, 1058, [arXiv:2007.06333].

[47] K. Saurabh and K. Jusufi, Eur. Phys. J. C **81**, 490 (2021) [arXiv:2009.10599].

[48] C. Bambi, K. Freese, S. Vagnozzi and L. Visinelli, Phys. Rev. D **100**, 044057 (2019).

[49] S. Vagnozzi and L. Visinelli, Phys. Rev. D **100**, no. 2, 024020 (2019) [arXiv:1905.12421].

[50] S. Haroon, K. Jusufi and M. Jamil, Universe **6**, no. 2, 23 (2020) [arXiv:1904.00711].

[51] R. Shaikh and P. S. Joshi, JCAP **1910**, 064 (2019) [arXiv:1909.10322].

[52] P. V. P. Cunha, C. A. R. Herdeiro and E. Radu, Universe **5**, no. 12, 220 (2019) [arXiv:1909.08039].

[53] I. Banerjee, S. Chakraborty and S. SenGupta, Phys. Rev. D **101**, no. 4, 041301 (2020) [arXiv:1909.09385].

[54] X. H. Feng and H. Lu, Eur. Phys. J. C **80**, no. 6, 551 (2020) [arXiv:1911.12368].

[55] S. F. Yan, C. Li, L. Xue, X. Ren, Y. F. Cai, D. A. Easson, Y. F. Yuan and H. Zhao, Phys. Rev. Res. **2**, no. 2, 023164 (2020) [arXiv:1912.12629].

[56] A. Allahyari, M. Khodadi, S. Vagnozzi and D. F. Mota, JCAP **2002**, 003 (2020) [arXiv:1912.08231].

[57] M. Rummel and C. P. Burgess, JCAP **2005**, 051 (2020) [arXiv:2001.00041].

[58] S. Vagnozzi, C. Bambi and L. Visinelli, Class. Quant. Grav. **37**, no. 8, 087001 (2020) [arXiv:2001.02986].

[59] M. Khodadi, A. Allahyari, S. Vagnozzi and D. F. Mota, JCAP **2009**, 026 (2020) [arXiv:2005.05992].

[60] Z. Chang and Q. H. Zhu, Phys. Rev. D **102**, no. 4,

044012 (2020) [arXiv:2006.00685].
[61] S. I. Kruglov, Mod. Phys. Lett. A **35**, no. 35, 2050291 (2020) [arXiv:2009.07657].
[62] D. Ghosh, A. Thalapillil and F. Ullah, [arXiv:2009.03363].
[63] D. Psaltis *et al.* [Event Horizon Telescope Collaboration], Phys. Rev. Lett. **125**, no. 14, 141104 (2020) [arXiv:2010.01055].
[64] Z. Hu, Z. Zhong, P. C. Li, M. Guo and B. Chen, Phys. Rev. D **103**, no.4, 044057 (2021) [arXiv:2012.07022].
[65] C. Li, H. Zhao and Y. F. Cai, Phys. Rev. D **104**, no.6, 064027 (2021) [arXiv:2012.10888].
[66] J. D. Bekenstein, Phys. Rev. D **7**, 2333 (1973).
[67] S. W. Hawking, Commun. Math. Phys. **43**, 199 (1975).
[68] J. D. Barrow, Phys. Lett. B **808**, 135643 (2020) [arXiv:2004.09444].
[69] E. N. Saridakis, Phys. Rev. D **102**, 123525 (2020) [arXiv:2005.04115].
[70] E. N. Saridakis, JCAP **07**, 031 (2020) [arXiv:2006.01105].
[71] A. A. Mamon, A. Paliathanasis and S. Saha, Eur. Phys. J. Plus **136**, no.1, 134 (2021) [arXiv:2007.16020].
[72] Q. Huang, H. Huang, B. Xu, F. Tu and J. Chen, Eur. Phys. J. C **81**, 686 (2021).
[73] S. Rani and N. Azhar, Universe **7**, 268 (2021).
[74] P. Adhikary, S. Das, S. Basilakos and E. N. Saridakis, Phys. Rev. D **104**, no.12, 123519 (2021) [arXiv:2104.13118].
[75] A. Sheykhi, Phys. Rev. D **103**, 123503 (2021) [arXiv:2102.06550].
[76] E. M. C. Abreu and J. A. Neto, [arXiv:2107.04869].
[77] U. K. Sharma, G. Varshney and V. C. Dubey, Int. J. Mod. Phys. D **30**, 2150021 (2021) [arXiv:2012.14291].
[78] A. Lymperis, S. Basilakos and E. N. Saridakis, Eur. Phys. J. C **81**, no.11, 1037 (2021) [arXiv:2108.12366].
[79] N. Drepanou, A. Lymperis, E. N. Saridakis and K. Yesmakhanova, [arXiv:2109.09181].
[80] E. C. Telali and E. N. Saridakis, [arXiv:2112.06821].
[81] E. M. C. Abreu and J. A. Neto, Phys. Lett. B **810**, 135805 (2020) [arXiv:2009.10133].
[82] E. M. C. Abreu and J. A. Neto, Eur. Phys. J. C **80**, 776 (2020).
[83] E. M. C. Abreu, J. A. Neto and E. M. Barboza, jr., EPL **130**, 40005 (2020) [arXiv:2005.11609].
[84] S. Nojiri, S. D. Odintsov and V. Faraoni, [arXiv:2109.05315].
[85] S. Chandrasekhar, *The mathematical theory of black holes*, Oxford University Press, Oxford (2002).
[86] M. Khodadi and E. N. Saridakis, Phys. Dark Univ. **32**, 100835 (2021) [arXiv:2012.05186].
[87] K. Jusufi, Phys. Rev. D **101**, 084055 (2020) [arXiv:1912.13320].
[88] B. Cuadros-Melgar, R. D. B. Fontana and J. de Oliveira, Phys. Lett. B **811**, 135966 (2020) [arXiv:2005.09761].
[89] R. Narayan, M. D. Johnson and C. F. Gammie, Astrophys. J. Lett. **885**, no.2, L33 (2019) [arXiv:1910.02957].
[90] X. X. Zeng, H. Q. Zhang and H. Zhang, Eur. Phys. J. C **80**, no.9, 872 (2020) [arXiv:2004.12074].
[91] H. Falcke, F. Melia and E. Agol, Astrophys. J. Lett. **528**, L13 (2000) [arXiv:astro-ph/9912263].
[92] C. Bambi, Phys. Rev. D **87**, 107501 (2013) [arXiv:1304.5691].
[93] S. Gillessen, F. Eisenhauer, T. K. Fritz, H. Bartko, K. Dodds-Eden, O. Pfuhl, T. Ott and R. Genzel, Astrophys. J. Lett. **707**, L114-L117 (2009) [arXiv:0910.3069].
[94] R. Abuter *et al.* [GRAVITY], Astron. Astrophys. **615**, L15 (2018) [arXiv:1807.09409].
[95] J. L. Walsh, A. J. Barth, L. C. Ho and M. Sarzi, Astrophys. J. **770** (2013), 86
[96] M. Shahzadi, M. Kološ, Z. Stuchlík, Y. Habib, arXiv:2201.04442
[97] T. Do, A. Hees, A. Ghez, G. D. Martinez, D. S. Chu, S. Jia, S. Sakai, J. R. Lu, A. K. Gautam and K. K. O'Neil, *et al.* Science **365**, no.6454, 664-668 (2019) [arXiv:1907.10731].
[98] E. A. Becerra-Vergara, C. R. Arguelles, A. Krut, J. A. Rueda and R. Ruffini, Astron. Astrophys. **641**, A34 (2020) [arXiv:2007.11478].
[99] S. Nampalliwar, S. Kumar, K. Jusufi, Q. Wu, M. Jamil and P. Salucci, Astrophys. J. **916**, no.2, 116 (2021) [arXiv:2103.12439].
[100] K. Jusufi, S. Kumar, M. Azreg-Aïnou, M. Jamil, Q. Wu and C. Bambi, [arXiv:2106.08070].
[101] F. K. Anagnostopoulos, S. Basilakos and E. N. Saridakis, Eur. Phys. J. C **80**, 826 (2020) [arXiv:2005.10302].
[102] G. Leon, J. Magaña, A. Hernández-Almada, M. A. García-Aspeitia, T. Verdugo and V. Motta, [arXiv:2108.10998].
[103] J. D. Barrow, S. Basilakos and E. N. Saridakis, Phys. Lett. B **815** (2021), 136134 [arXiv:2010.00986].
[104] G.F.R. Ellis, R. Maartens and M.A.H. MacCallum, *Relativistic Cosmology* Cambridge University Press (2012).
[105] M. Azreg-Aïnou, black Eur. Phys. J. C **77**, no.1, 36 (2017) [arXiv:1605.06063].
[106] A. K. Ahmed, M. Azreg-Aïnou, M. Faizal and M. Jamil, black Eur. Phys. J. C **76**, no.5, 280 (2016) [arXiv:1512.02065].
[107] M. Azreg-Aïnou, A. K. Ahmed and M. Jamil, Class. Quant. Grav. **35**, no.23, 235001 (2018) [arXiv:1809.03320].
[108] S. Bahamonde and M. Jamil, Eur. Phys. J. C **75**, 508 (2015) [arXiv:1508.07944].
[109] A. K. Ahmed, U. Camci and M. Jamil, Class. Quant. Grav. **33**, no.21, 215012 (2016) [arXiv:1610.01129].
[110] A. Aslam, M. Jamil and R. Myrzakulov, Phys. Scripta **88**, 025003 (2013) [arXiv:1308.0325].
[111] S. Weinberg, *Gravitation and Cosmology* John Wiley and Sons (1972).
[112] R. Kumar, S. U. Islam and S. G. Ghosh, Eur. Phys. J. C **80**, no.12, 1128 (2020) [arXiv:2004.12970].
[113] G. Fragione and A. Loeb, ApJL **901**, no.2, L32 (2020) [arXiv:2008.11734].